DESIGN AND NUMERICAL ANALYSIS OF PROCESSES IN SILOXANE VAPOR DRIVEN TURBINE

A. Sebelev*[1], R. Scharf[2], N. Zabelin[1], M. Smirnov[1]

[1]Peter the Great St. Petersburg Polytechnic University (SPbPU),
Department "Turbines, Hydro machines and aero-engines"
St. Petersburg, Russia;
[2]Leibniz Universität Hannover,
Institut für Kraftwerkstechnik und Wärmeübertragung
Hannover, Germany
e-mail: a.sebelev.turbo@mail.ru

ABSTRACT

The problem of decreasing of fossil fuel consumption and energy efficiency is one of today's major conceptions in the field of energy economics. Waste heat recovery is one of the promising solutions for this problem. One of the ways to increase efficiency of the waste heat recovery process is using siloxanes as working fluids for organic Rankine cycles (ORC).

SPbPU scientists have analyzed peculiarities of the steady-state expansion process in the siloxane vapor driven turbine. The design of the nozzle and the blade wheel of the turbine is supersonic due to the low speed of sound of siloxanes. Initial parameters of siloxane were subcritical; a pressure ratio of the turbine was 25. Progressive steps of the initial temperature, pressure ratio and rotational velocity were used to obtain convergence of the solution process. The changings of positions of the nozzle and blade wheel critical sections were established. The details of the supersonic vortices interaction in the blade wheel flow range were analyzed.

The efficiency and power output of the investigated turbine stage were estimated as 0.699 and 309.1 kW, respectively.

1. INTRODUCTION

Waste heat recovery is one of the promising solutions to increase efficiency of different plants and industrial processes (Larjola (1995), Vescovo (2009)). The highest volume of waste heat resources takes place at different thermal power plants, cement, metallurgical and chemical productions. In Russia it is also the gas transport industry. The estimation of waste heat thermal power at the all gas compressor stations of "Gazprom" is 87.9 GW (Lykov *et al.* (2013)). Rough estimations of waste heat thermal power at different productions in Russia, made on the base of Key World Energy Statistics (2014), are: 3.9 GW at the all cement production plants, 2.8 GW at the all metallurgical production plants and 1.9 GW at the all chemical production plants. In the other words, all this waste heat may be turned to 14.5 GW of electrical power by the most conservative estimate.

In most cases using of organic Rankine cycles (ORC) for recovery plants provides higher efficiency of the recovery plants in comparison with water steam Rankine cycle due to low temperature levels of the waste heat streams (Larjola (1995), Hung *et al.* (1997), Vescovo (2009)). The average temperature level of the waste heat streams in the whole Russian gas transport system is 390ºC by the estimation of Lykov *et al.* (2013). The average temperature level of the waste heat streams at other productions in Russia varies from 150ºC to 350ºC. One of the most important questions in the recovery plant designing is the choosing of a working fluid. Nowadays the aspects of using of various hydrocarbons, freons and alcohols in ORC are widely researched by different authors (Iqbal *et al.* (1977), Hung *et al.* (1997), Shuster *et al.* (2010), Gao *et al.* (2012)). Modern requirements for environment safety determine ozone depletion potential (ODP) and global warming potential (GWP) as main criteria for

choosing of a working fluid. It was shown that in this case the most promising alternatives to different hydrocarbons, freons and alcohols are zeotropic mixtures and siloxanes (Heberle *et al.* (2012), Chys *et al.* (2012), Weith *et al.* (2014)). The aspects of using of siloxanes in ORC were investigated by Lai *et al.* (2011), Fernandez *et al.* (2011), Uusitalo *et al.* (2013). It was shown that in this case the efficiency of ORC may be increased up to 23 – 25%.

The turbines for organic working fluids have essential differences in details of the expansion process in comparison with typical gas and steam turbines. The special supersonic design is required for such turbines due to low speed of sound of different organic working fluids. The aspects of designing of the ORC driven turbines were outlined by different authors. Yamamoto *et al.* (2001) designed and tested R-123 centripetal turbine; Kang (2012) designed and tested R-245fa radial-inflow turbine; Casati *et al.* (2014) described designing method of the ORC centrifugal microturbines. Guardone *et al.* (2013) described the influence of molecular complexity on nozzle design.

Despite the high volume of investigations in the area of organic working fluids expansions the peculiarities of siloxanes behavior during the expansion process still haven't been outlined. Thus, the scope of the present paper is to investigate the siloxane expansion process and to outline its peculiarities.

2. INVESTIGATION OBJECT

2.1. Initial parameters of the expansion process

Hexametyldisiloxane (MM) was chosen as working fluid for the expansion process. The initial pressure p_0 was set as 1 MPa. The initial temperature T_0 was set as a vapor saturation temperature at chosen initial pressure. The turbine pressure ratio has been chosen as 25 to provide the required turbine enthalpy drop upon the condition of 300 kW power output of the turbine stage. Trans- and supercritical initial parameters were not considered.

Positive slope of MM vapor saturation curve provides inability of intersection between expansion process curve and two-phase region as shown in figure 1. It means that there is no possibility of droplet formation in the turbine stage.

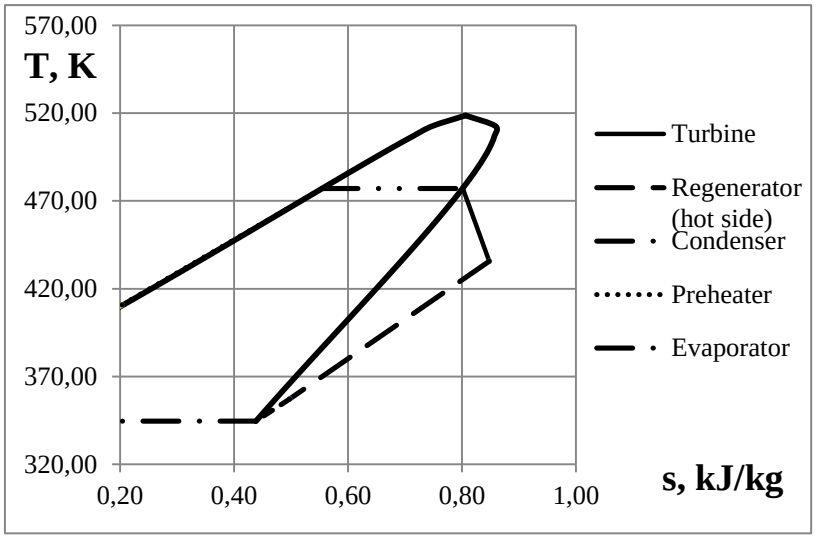

Figure 1: T-s diagram of the expansion process

2.2. The turbine

A single-stage double-flow axial turbine was chosen as the expander machine. The choice of the double-flow design was made due to high axial forces acting on the turbine rotor. The subsonic part of the nozzle was designed according to Vitoshinski profile. The supersonic part of the nozzle was designed using the SPbPU high pitch-chord ratio design. The main features of the high pitch-chord ratio design, described in details by Rassokhin (2004), are:

- small angles α_1 (3..5º) and β_1 (8..14º);

- high blade wheel flow turning angle (Ω = 151..164º);
- high pitch-chord ratio for the nozzle and blade wheel blades (t_N/b_N > 4, t_{BW}/b_{BW} > 1.1);
- high enthalpy drops at one turbine stage (up to 800 kJ/kg).

The supersonic blade profile C9022B was chosen for the blade wheel. This blade profile was described in details by Dejch *et al.* (1965). The reason to use blade profile with thick leading edge is strong changing of MM properties with relation to thermodynamic parameters. The design of the nozzle and blade wheel is supersonic due to low MM speed of sound. Involutions of the nozzle and blade wheel at the mean diameter are shown in figure 2. The blade wheel of the turbine has a tip shroud. The main geometric parameters of the single-flow turbine stage are given in table 1.

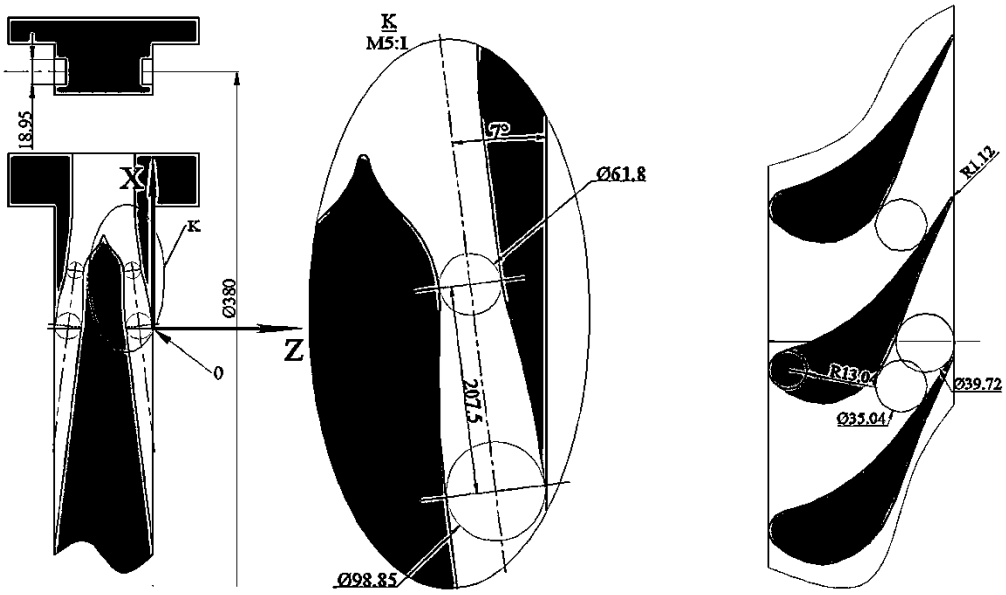

a) b)

Figure 2: Involutions of the nozzle (a) and blade wheel (b) at the mean diameter

Table 1: The main geometric parameters of the one-flow turbine stage

Parameter	Dimensions	Value	Parameter	Dimensions	Value
D_m	mm	380	α_1	deg.	7.00
n	rev/min	12000	ΔL_{ax}	mm	7.00
H_0	kJ/kg	66.26	ΔL_{tc}	mm	0.30
G	kg/s	6.86	β_1	deg.	90.00
C_{ax}/u	-	1.52	Z_2	-	55
ε	-	0.97	l_2	mm	24.75
Z_1	-	7	β_2^*	deg.	30.00
l_1	mm	18.95	Ω	deg.	60.00

3. NUMERICAL SIMULATION METHOD

The SPbPU method for numerical simulation of processes in supersonic turbines, described by Zabelin *et al.* (2013), was used. ANSYS CFX was used to provide the numerical simulation.

The original relation between the number of nozzles and number of working blades is 7/55. The relation 1/8 and periodic boundary conditions were used in the computational model. This assumption is correct to be used with Frozen Rotor interface between the nozzle and blade wheel areas because the relation between connecting areas in this case is 1:1.018. The modeling of blade wheel tip shroud was also considered in numerical model in assumption of rotating motion of tip shroud domain. The computational model of the single-flow turbine stage is presented in figure 3.

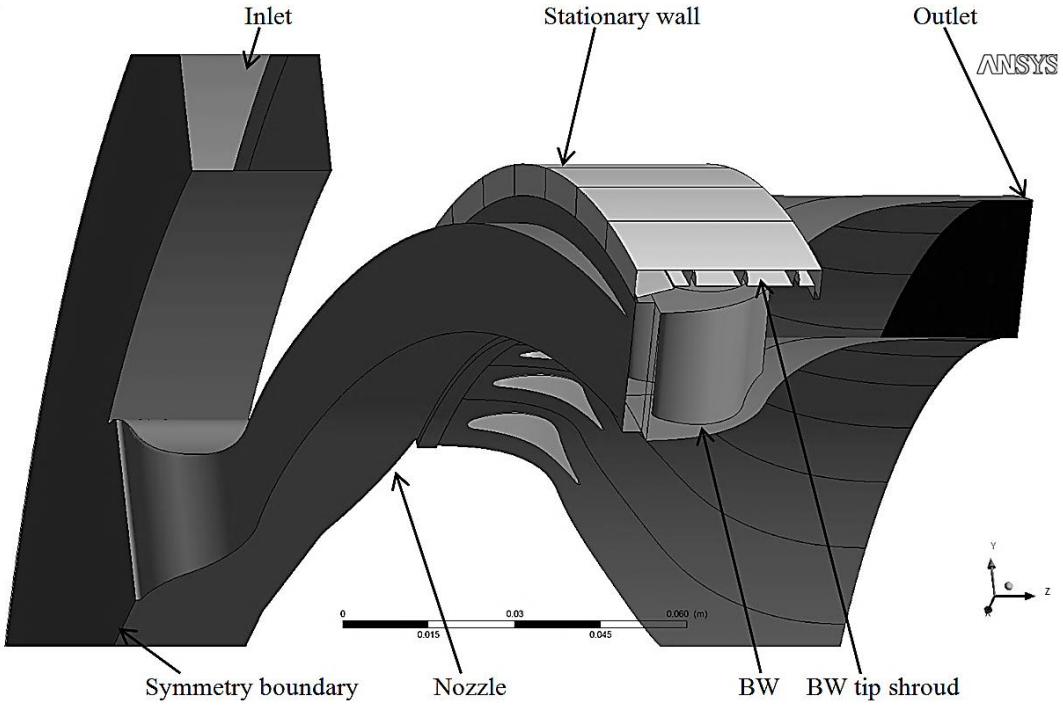

Figure 3: Computational model of the single-flow turbine stage

High-Reynolds version of the k-ω SST turbulence model was used. Steady-state Frozen rotor interface between the nozzle and blade wheel areas was used to model rotor-stator interaction. Flow parameters of the turbine stage were obtained by averaging of their values for 4 positions of blade wheel relatively to the nozzle in the range of blade wheel pitch angle.

Aungier Redlich Kwong real gas equation of state was used to model thermodynamic properties of MM during the expansion process. The main parameters need to be specified are: molar mass, critical temperature and pressure, acentric factor and boiling temperature. Zero pressure polynomial coefficients were obtained with using REFPROP databases to evaluate specific heat capacity of MM. Kinetic Theory models were used to model transport properties of MM. Rigid Non Interacting Sphere model was used to model MM dynamic viscosity behavior.

Total parameters at inlet (p_0 = 1 MPa, T_0 = 477.1 K) and static pressure at outlet (p_0 = 0.04 MPa) were specified as boundary conditions in computational model. Progressive steps of the boundary conditions were used to obtain convergence of the solution process. The iteration steps between the changings of boundary conditions were different to decrease their negative influence on the solution process. Monitoring of the RMS residuals, imbalances and turbine efficiency and power output were used to control convergence of the solution process. The criteria of the convergent solution in present research were:

- drop of the RMS residuals more than 10^2;
- imbalances less than 0.5%;
- fluctuation of the turbine efficiency and power output less than 5%.

Three different types of computational domains discretization were compared to obtain grid independent solution. The results of the grid independency study are presented in table 2.

Table 2: The results of the grid independency study

Grid type	1 nozzle sector, millions of nodes	8 blade wheel sectors, millions of nodes	8 tip shroud sectors, millions of nodes	Difference in the turbine efficiency with the previous grid, %	Difference in the turbine power output with the previous grid, %
Coarse	0.68	3.21	3.15	-	-
Medium	1.15	6.85	4.26	10.2	15.4
Fine	1.98	10.64	5.32	4.2	4.8

The medium grid was used in further calculations. The grid structure is presented in figure 4.

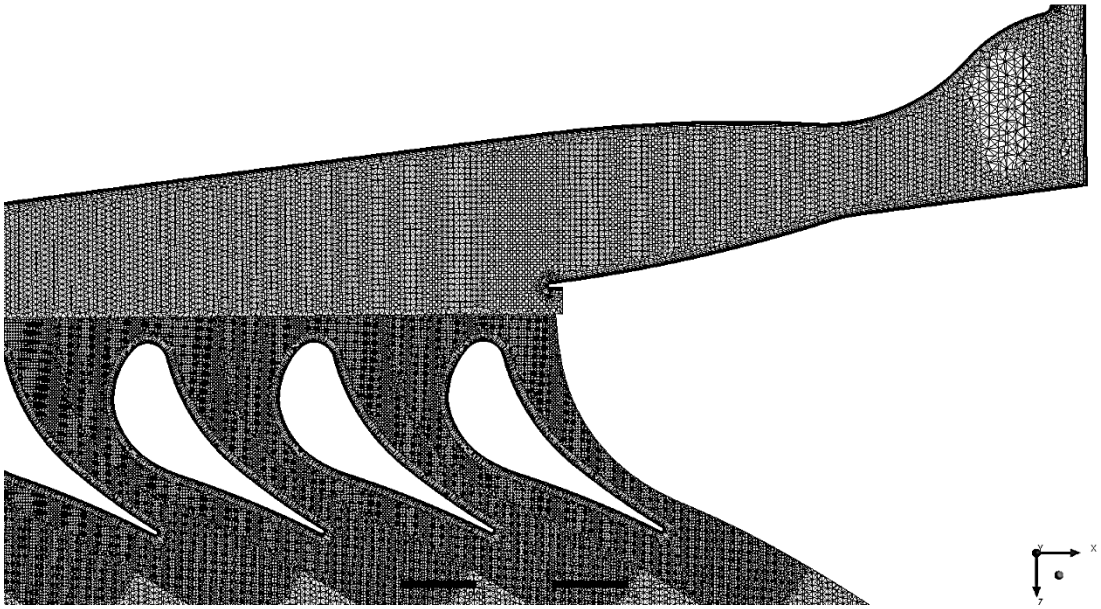

Figure 4: The grid structure

4. DISCUSSION OF THE RESULTS

The values of the calculated thermodynamic and transport properties were compared with the values obtained with using REFPROP databases to estimate tolerance of the obtained results. Maximum deviation between CFX and REFPROP results was less than 5% for specific heat capacity and dynamic viscosity. It is noteworthy that isentropic exponent of MM has a strong nonlinear dependence on temperature and pressure in superheated vapor area as shown in figure 5a. In this case it is incorrect to use constant isentropic exponent in preliminary turbine calculations. Rough boundary in figure 5a is a consequence of discrete steps of temperature and pressure.

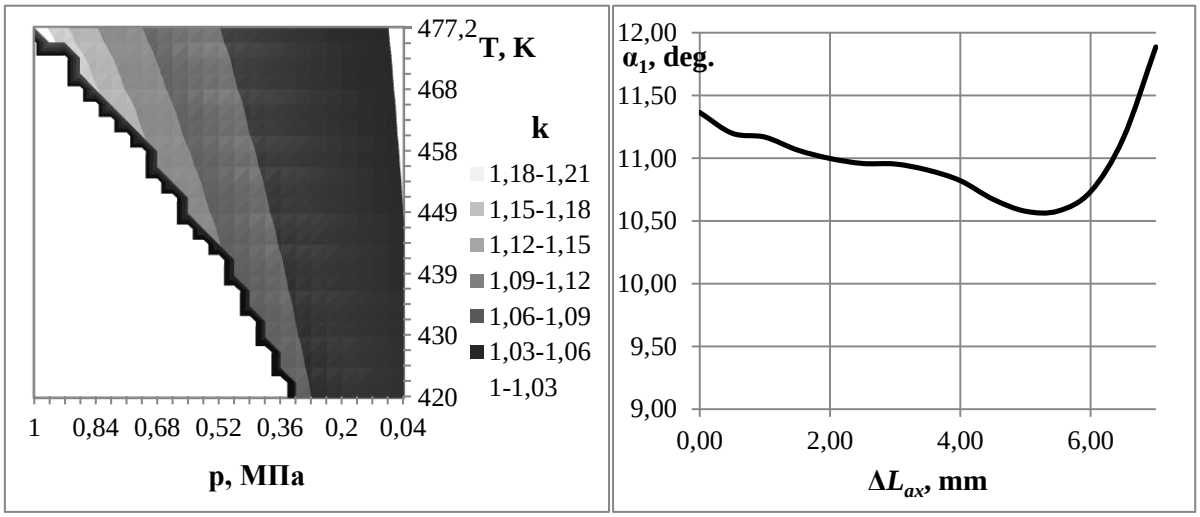

a) b)

Figure 5: MM isentropic exponent dependence on temperature and pressure in superheated vapor area (a) and varying of the nozzle outlet angle outbound of the nozzle (b)

The analysis of Mach number field in the nozzle (figure 6) shows that the flow in the critical section is not fully supersonic. It can be seen in details in figure 7. Physically, it means that the position of real critical section changed to the downstream direction in comparison with its design position. This

phenomenon was established by Reichert and Simon (1997). This fact means that the theoretical mass flow rate through the supersonic nozzle, defined as:

$$G_t = \frac{p_0 \cdot S_{cs}}{\sqrt{T_0}} \sqrt{\frac{k}{R}\left(\frac{2}{k+1}\right)^{\frac{k+1}{k-1}}}, \tag{1}$$

should be based on the cross-sectional area of the real critical section. Additionally, the velocity profile near the critical section is highly distorted towards to the straight nozzle wall. This is a consequence of the non-symmetric shape of the nozzle and was also outlined by Reichert and Simon (1997). The same situation takes place near the blade wheel critical section.

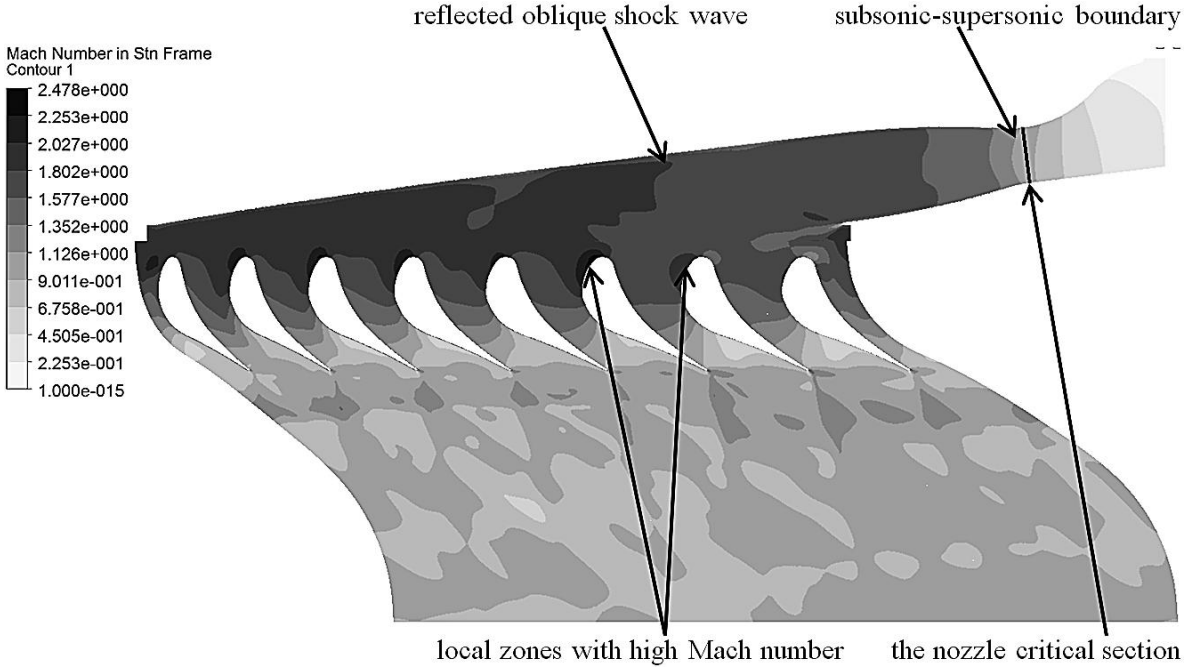

Figure 6: Mach number field in the turbine stage at the mean diameter

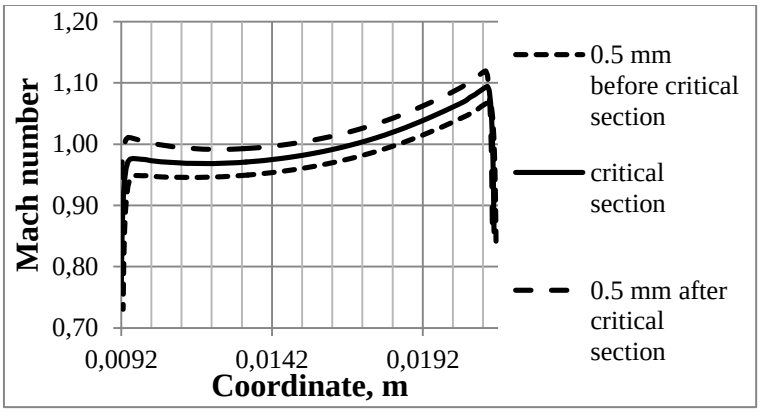

Figure 7: Velocity profiles near the nozzle critical section at the mean diameter

The oblique shock wave from the nozzle reflects from the nozzle wall and then impinges on the leading edge of the blades. This leads to the appearing of the local zones with high Mach number (up to 2.5 in stationary frame) at the blades leading edges. Such flow behavior is typical for axial supersonic turbines and was described in details by Kirillov (1972) and Traupel (1977). It should be outlined that the nozzle outlet angle, defined as:

$$\alpha_1 = arctg\left(\frac{G \cdot D_m \cdot c_{1z}}{2M_N}\right), \tag{2}$$

has a decreasing value outbound of the nozzle as shown in figure 5b. Zabelin *et al.* (2013) showed that this phenomenon is a consequence of the blade wheel influence on the nozzle in trans- and supersonic turbines. The nozzle torque in equation (2) was calculated directly in CFD-Post.

The analysis of the flow structure in the blade wheel shows that double vortex structure appears at the blade wheel inlet as shown in figure 8. It is a consequence of complex phenomena which take place at the edges of the nozzles active flow sectors. These phenomena related to the flow separation and were described by Natalevich (1979). The hub vortex rotates clockwise and rests against the blade wheel hub. The shroud vortex has a counterclockwise rotation and rests against the blade wheel shroud because of the inertial forces. This flow separation leads to additional energy loses at the boundary of vortices interaction as shown in figure 9.

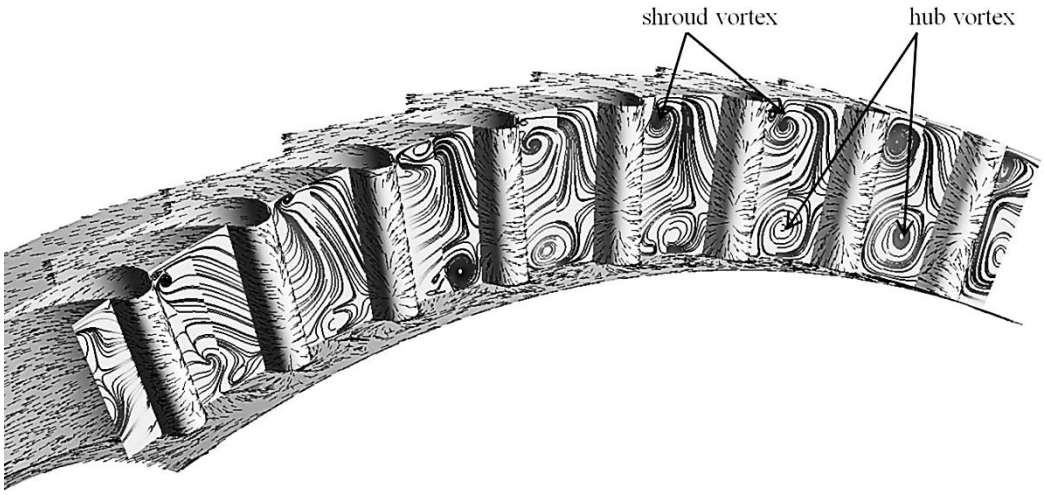

Figure 8: Flow structure at the blade wheel inlet

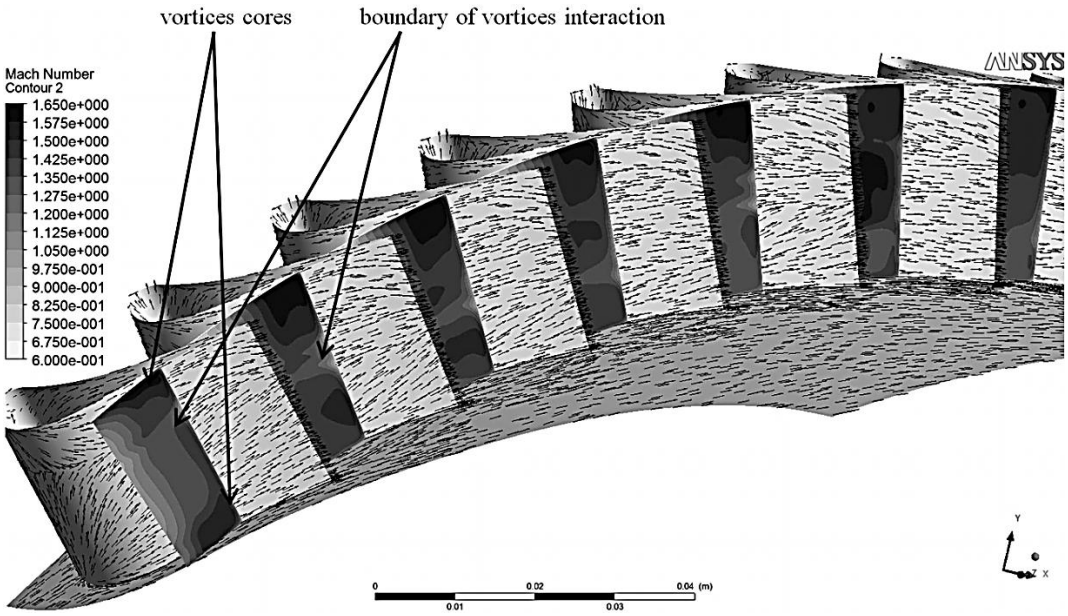

Figure 9: Flow structure at the blade wheel outlet

Another peculiarity that should be highlighted is a specific shape of the shock wave after the blade wheel. As it can be seen in figures 8 and 9 the hub vortex increases as it drew in the blade wheel flow range. This leads to the decreasing of the shroud vortex and increasing of the Mach number at the blade wheel shroud. This process is illustrated in figures 9 and 10. The zones with low velocities at the blade wheel shroud in figure 10 are the zones of the tip shroud leakage interaction with the main flow. High volume of the hub vortex together with strong dependence of the MM density on thermodynamic parameters leads to appearing of the normal shock wave at the blade wheel outlet as

shown in figure 10. The intensity of the normal shock wave decreases from hub to shroud due to low volume of the shroud vortex in comparison with the hub vortex. This is also the reason for the high Mach number zones appearing at the blade wheel shroud. The volume of the high Mach number zones increases with distance from the blade wheel. It means that shroud vortex is underexpanded and continues its expansion after the blade wheel.

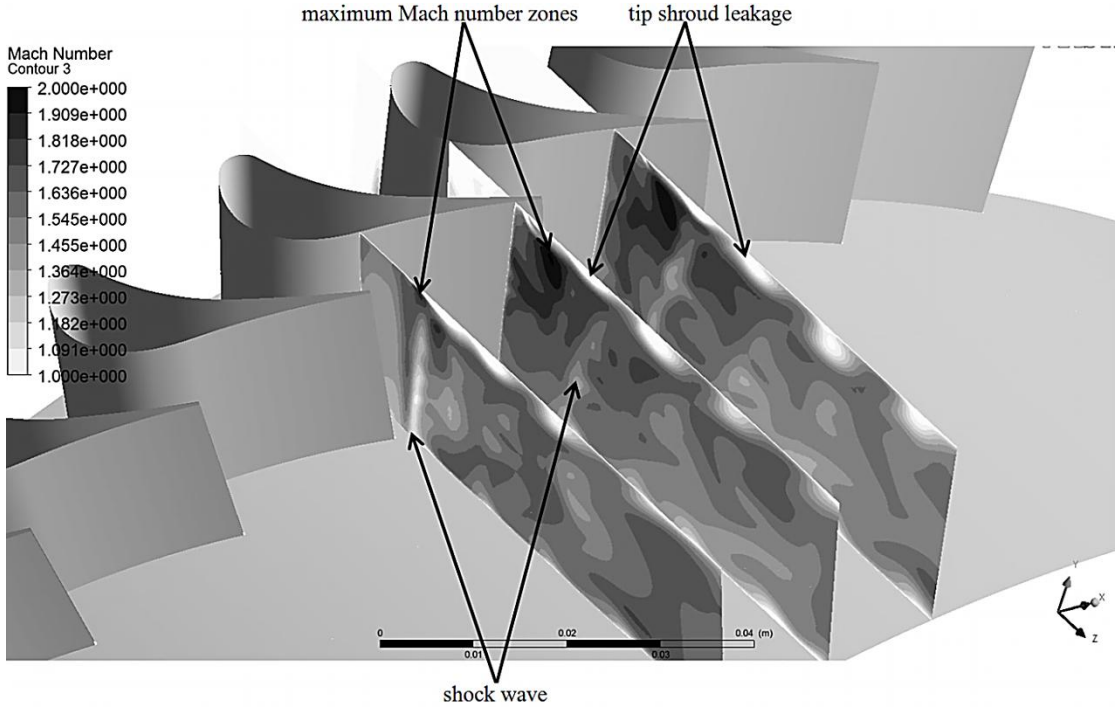

Figure 10: Shock wave at the blade wheel outlet

The efficiency and power output of the investigated turbine stage were calculated with using following equations:

$$\eta_i = \frac{M_{BW} \cdot \pi \cdot n}{30 \cdot G \cdot H_0}, \tag{3}$$

$$N = \frac{M_{BW} \cdot \pi \cdot n}{30}. \tag{4}$$

The calculated values of the efficiency and power output for investigated single-flow turbine stage are 0.699 and 309.1 kW respectively.

5. CONCLUSIONS

The expansion process in the siloxane vapor driven turbine was modeled. The peculiarities of the siloxane expansion process were outlined. The important conclusions about the calculations of theoretical mass flow rate through the supersonic nozzles were made. It was shown that in case of the supersonic nozzles the equation for theoretical mass flow rate should be based on the cross-sectional area of the real critical section. It was also shown that it is inacceptable to use constant isentropic exponent in case of the preliminary ORC turbines calculations.

Most of the outlined peculiarities are typical for the supersonic axial microturbines because of subcritical initial parameters of the siloxane vapor. However, the strong relation of the siloxane properties to the thermodynamic parameters determines its nonconventional behavior during the expansion in the blade wheel. Complex interaction between two supersonic vortices in the blade wheel leads to additional energy losses and appearing of the normal shock wave after the blade wheel. As a result, calculated efficiency of the investigated turbine stage is 0.699. This value is close to the efficiency of the water steam microturbines with mean diameter up to 500 mm.

NOMENCLATURE

GW	Gigawatt	
GWP	Global Warming Potential	
kW	Kilowatt	
MM	Hexametyldisiloxane	
ODP	Ozone Depletion Potential	
ORC	Organic Rankine Cycle	
SPbPU	Peter the Great St. Petersburg Polytechnic University	
C_{ax}/u	stage load coefficient	
c_{1z}	axial component of velocity at the nozzle outlet	m/s
D_m	mean diameter	m
G	mass flow rate	kg/s
H_0	isentropic enthalpy drop	kJ/kg
k	isentropic exponent	
l_1	nozzle height	mm
l_2	blade height	mm
M	torque	N·m
n	rotational speed	rev/min
p_0	nozzle inlet pressure	MPa
p_2	blade wheel outlet pressure	MPa
R	individual gas constant	J/(kg·K)
S	cross-sectional area	m^2
T_0	nozzle inlet temperature	K
Z_1	number of nozzles	
Z_2	number of blades	
α_1	nozzle outlet angle	deg.
β_1	blade wheel inlet angle in relative frame	deg.
β_2^*	blade wheel outlet angle in relative frame	deg.
ΔL	clearance value	mm
ε	partial admission ratio	

Subscript

BW	blade wheel
N	nozzle
ax	axial
cs	critical section
i	internal
t	theoretical
tc	tip clearance

REFERENCES

[1] Casati, E., Vitale, S., Pini, M., Persico, G., Colonna, P., 2014, Centrifugal turbines for mini-organic Rankine cycle power systems, *Journal of Engineering for Gas Turbines and Power*, vol. 136, 122607.

[2] Chys, M., van den Broek, M., Vanslambrouck, B., De Paepe, M., 2012, Potential of zeotropic mixtures as working fluids in organic Rankine cycles, *Energy*, vol. 44, pp. 623 – 632.

[3] Dejch, E.M., Filipov, A.G., Lazariev, J.L., 1965, *Atlas profilej reshetok osevyh turbin*, Mashinostroyenie, Moscow, 96p.

[4] Fernandez, F.J., Prieto, M.M., Suarez, I., 2011, Thermodynamic analysis of high-temperature regenerative organic Rankine cycles using siloxanes as working fluids, *Energy*, vol. 36, pp. 5239 – 5249.

[5] Gao, H., Liu, Ch., He, Ch., Xu, Xi., Wu, Sh., Li, Y., 2012, Performance Analysis and Working Fluid Selection of a supercritical Organic Rankine Cycle for low grade waste heat recovery, *Energies*, vol. 5, pp. 3233 – 3247.

[6] Guardone, A., Spinelli, A., Dossena, V., 2013, Influence of molecular complexity on nozzle design for an organic vapor wind tunnel, *Journal of Engineering for Gas Turbines and Power*, vol. 135, 042307.

[7] Heberle, F., Preißinger, M., Brüggemann, D., 2012, Zeotropic mixtures as working fluids in Organic Rankine Cycles for low-enthalpy geothermal resources, *Renewable Energy*, vol. 37, pp. 364 – 370.

[8] Hung, T.C., Shai, T.Y., Wang, S.K., 1997, A review of Organic Rankine Cycles (ORCs) for the recovery of low-grade waste heat, *Energy*, vol. 22, pp. 661 – 667.

[9] Iqbal, K.Z., Fish, L.W., Starling, K.E., 1977, Isobutane geothermal binary cycle sensitivity analysis, Proceedings *Oklahoma Academic Science*, The University of Oklahoma, pp. 131 – 137.

[10] Kang, S.H., Design and experimental study of ORC (organic Rankine cycle) and radial turbine using R245fa working fluid, 2012, *Energy*, vol. 41, pp. 514 – 524.

[11] Key World Energy Statistics, *International Energy Agency*, 2014.

[12] Kirillov, I.I., 1972, *Teorija turbomashin*, Mashinostroyenie, Leningrad, 533p.

[13] Lai, N.A., Wendland, M., Fischer, J., 2011, Working fluids for high-temperature organic Rankine cycles, *Energy*, vol. 36, pp. 199 – 211.

[14] Larjola, J., 1995, Electricity from industrial waste heat using high-speed organic Rankine cycle (ORC), *International journal of production economics*, vol. 41, pp. 227 – 235.

[15] Lykov, A.V., Zabelin, N.A., Rassokhin, V.A., 2013, Estimation of waste heat resources in Russian unified system of gas supply, *St. Petersburg State Polytechnical University Journal*, vol. 183 (4), pp. 136–145.

[16] Natalevich, A.S., 1979, *Vozdushnye mikroturbiny*, Mashinostroyenie, Moscow, 192p.

[17] Rassokhin, V.A., 2004, Turbiny konstrukcii LPI: preimushhestva, harakteristiki, opyt razrabotki i primenenie, *St. Petersburg State Polytechnical University Journal*, vol. 491, pp. 152 – 161.

[18] Reichert, A.W., Simon, H., 1997, Design and flow field calculations for transonic and supersonic radial inflow turbine guide vanes, *Journal of turbomachinery*, vol. 119 (1), pp. 103 – 113.

[19] Shuster, A., Karellas, S., Aumann, R., 2010, Efficiency optimization potential in supercritical Organic Rankine Cycles, *Energy*, vol. 35, pp. 1033 – 1039.

[20] Traupel, W., 1977, *Thermische Turbomaschinen*, 3. Aufl., Springer, Berlin, 579p.

[21] Uusitalo, A., Turunen-Saaresti, T., Honkatukia, J., Colonna, P., Larjola, J., 2013, Siloxanes as working fluids for mni-ORC systems based on high-speed turbogenerator technology, *Journal of Engineering for Gas Turbines and Power*, vol. 135, 042305.

[22] Vescovo, R., 2009, ORC recovering industrial heat, *Cogeneration and On-Site Power Production*, vol. 2, pp. 53 – 57.

[23] Weith, T., Heberle, F., Preißinger, M., Brüggemann, D., 2014, Performance of siloxane mixtures in a high-temperature Organic Rankine Cycle considering the heat transfer characteristics during evaporation, *Energies*, vol. 7, pp. 5548 – 5565.

[24] Yamamoto, T., Furuhata, T., Arai, N., Mori, K., 2001, Design and testing of the organic Rankine cycle, *Energy*, vol. 26, pp. 239 – 251.

[25] Zabelin, N.A., Rakov, G.L., Rassokhin, V.A., Sebelev, A.A., Smirnov, M.V., 2013, Investigation of fluid flow highlights in low flow-rated LPI turbine stages, *St. Petersburg State Polytechnical University Journal*, vol. 166 (1), pp. 45–53.